Contract No:

This document was prepared in conjunction with work accomplished under Contract No. DE-AC09-08SR22470 with the U.S. Department of Energy (DOE) Office of Environmental Management (EM).

Disclaimer:

U.S. DEPARTMENT OF ENERGY | Office of Science

Hybrid Magnetic Core-Shell Nanophotocatalysts for Environmental Applications

Patrick Gaulden[1] and Simona Hunyadi Murph, Ph.D.[1,2]

[1]Savannah River National Laboratory, Aiken SC 29808, U.S.A.
[2]Department of Physics and Astronomy, University of Georgia, Athens, GA, USA

ABSTRACT:

This research study describes a facile sol-gel method to creating hybrid iron (III) oxide/silica/titania nanomaterials decorated with gold nanoparticles for use in environmental applications. The multi-functional composition of the nanomaterials allows for photocatalyzed reactions to occur in both the visible and the UV range. The morphologies, elemental composition, and surface charge of the nanoparticles were determined by Scanning Electron Microscopy (SEM), Energy Dispersive X-ray Spectroscopy (EDS), and Phase Analysis Light Scattering (PALS), respectively. The photocatalytic activity of the synthesized hybrid nanoparticles for breaking down a model analyte, methyl orange (MO), was then evaluated using UV-Vis Spectroscopy. The efficiency of the photocatalyst under UV light irradiation was measured and compared to other well-studied nanophotocatalysts, namely titanium oxide and iron oxide nanoparticles. The concentration dependence of both the photocatalyst and the analyte was also investigated. By utilizing the known UV-active properties of TiO_2, the magnetic properties of Fe_2O_3, the optical properties of gold in the visible range of the spectrum, and the high stability of silica, a novel, highly efficient photocatalyst that is active on a broad range of the spectrum (UV-Vis) can be created to destroy organic pollutants in wastewater streams.

Keywords: nanotechnology, photocatalysis, gold, titania, silica, iron oxide, magnetic, environmental

I. INTRODUCTION

In recent years, nanophotocatalysts synthesized using noble metals and metal oxides have been the focus of many studies because of increasing demand for utilizing renewable energy sources, namely solar irradiation. Developing a method for efficiently using solar energy that is readily available worldwide can be a promising strategy for solving both environmental and energy related problems.[1] Many different materials and composites have been synthesized for environmental applications in hopes of creating a highly efficient photocatalyst with low toxicity, cost efficiency, and high stability.[2,3] Compared with bulk materials, nanomaterials bring a new dimension and efficiency to these environmental applications. Nanoscale materials have increased surface area and can be easily tuned to a specific size, leading to tailored properties for catalytic processes.[4] In addition to these properties, core-shell structures have been shown to

demonstrate synergistic properties, resulting in more effective catalysis than simply a mixture of the core and shell materials.[24] Nanophotocatalysts have been used to kinetically enhance a variety of reactions that either clean the environment, create a fuel, or both.[5,7,8] Specifically, photocatalysts used in advanced oxidation processes (AOP) can non-selectively degrade organic materials into carbon dioxide and water, demonstrating an application in wastewater treatment.[6] Landong et. al reported that the use of sub 10 nm titania nanoparticles could be used in the photocatalytic production of hydrogen gas for use in hydrogen fuel cell vehicles.[5] In this study, iron (III) oxide nanospheres (core) were purchased from Sigma-Aldrich and then a silica shell was synthesized around them. A titania shell was then further added and finally, the core-shell nanomaterials were decorated with gold nanospheres.

Titanium dioxide (TiO_2 or titania) has been known to be an exceptional photocatalyst in the UV range (E_g = 3.2 eV) for many reactions, from water splitting[5] to degradation of organic pollutants[7] and synthetic fuel production.[8] However, a much larger percentage of solar radiation is in the visible light range (approximately 40% is in the visible range, whereas only 4-5% is in the UV range),[23] greatly inhibiting the solar conversion efficiency of TiO_2. Several approaches have been taken to extend the wavelength range over which these nanomaterials are active. Methods include doping with non-metals and/or metals, or by combining TiO_2 with a lower band gap semiconductor to create a junction that decreases electron-hole pair recombination.[6]

Iron (III) oxide (Fe_2O_3 or magnetite), is also a well-studied nanocatalyst that is active in the visible range and has also received a great deal of attention because of its magnetic properties.[8] The band gap of magnetite is 2.2 eV, allowing the possibility of enhanced charge separation. Under visible light irradiation, the holes generated in the valence band of iron oxide could be maintained longer by the transfer of some electrons between the conduction bands of the two materials before recombination.[7] In addition, its magnetic properties allow it to be retrieved from the environment .[9] This minimizes the ecological footprint and creates a more economical catalyst through recycling.

While silica (SiO_2) is not catalytically active in the UV-Vis range, it acts as a stable foundation for titania, increasing its lifetime and efficiency.[10] By using a silica shell as a template, an additional titania shell can be formed on the exterior of the nanophotocatalysts that is both highly active and thermally and mechanically stable.

One of the most well-studied materials for extending titania's visible light photocatalytic properties is gold. In its bulk state, gold is relatively inert, but on the nanoscale interface, light is absorbed and scattered due to localized surface plasmon resonance (LSPR).[12] When gold nanoparticles are irradiated by light near its resonant wavelength, collective excitations of electrons within the metal are able to catalyze reactions.[25] These collective oscillations of electrons in the visible light range have been utilized in many applications, including solar cells[13] and surface enhanced spectroscopies, such as SERS.[14] In addition to having this unique property, gold nanoparticles have also been said to act as electron reservoirs for excited titania electrons, further increasing photocatalytic activity in the UV and visible range.[17] A possible setback for using gold as a catalyst is that it is less abundant metal and therefore is expensive. Murph et al. reported that the combination of gold nanoparticles with iron (III) oxide was more efficient in plasmonic heating applications than pure gold nanoparticles, allowing the use of gold to be more economically viable.[3]

While most studies utilize either metal or metal oxides to extend TiO_2's photocatalytic activity into the visible range (but not both), our study utilizes core-shell structure and plasmonic enhancement to increase photocatalytic efficiency. By combining many different non-toxic,

highly stable photocatalytic nanomaterials, a magnetic hybrid core-shell nanomaterial was synthesized and tested. The photocatalytic activity of the novel material was also compared to individual "benchmark" nanomaterials to determine efficiency in the breakdown of a model analyte, methyl orange.

II. EXPERIMENTAL

A. Materials

Chloroauric acid trihydrate, trisodium citrate, iron (III) oxide nanopowder (<50 nm), tetraorthosilicate, ethanol, aqueous ammonia (5N solution), High purity methyl orange (MO, chemical formula, $C_{14}H_{14}N_3NaO_3S$; CAS No. 547-58-0), and titanium (IV) *tert*-butoxide were purchased from Sigma Aldrich. All materials were used as received.

B. Synthetic procedure

1. Fe_2O_3-SiO_2 core-shell synthesis

Fabrication of the iron oxide silica core-shell nanoparticles followed a modified version of a previously reported sol-gel method.[15] A clean, sterile Falcon tube was rinsed with deionized (DI) water to be used for synthesis of iron (III) oxide/silica core-shell nanoparticles. A stock solution of Fe_2O_3 nanoparticles was prepared using 0.04 g of iron oxide (III) nanopowder (MW = 159.69 g mol^{-1}) with 10 mL DI water as solvent. 3 mL DI water was added to the tube using a pipette, followed by 100 µL of iron oxide nanoparticle solution. The solution was then sonicated for even dispersion. Then 5 mL of 3.4 mM sodium citrate solution (0.05 g in 50 mL water) was added. The solution was stirred for 1 h, and the nanoparticles were collected using a magnet and dispersed into 4mL of ethanol and 2 mL of 5 N aqueous ammonia. After an additional 30 min of stirring, 100 µL of tetraethyl orthosilicate (TEOS, MW = 208.33 g mol^{-1}) was added, followed by mechanical stirring for 4 h, and sonication for 15 min. The sample was separated from the supernatant by a magnet and washed several times before being dispersed in water. These particles were characterized by UV-Vis, Zeta potential/DLS, and SEM before adding the additional titania layer and gold nanoparticles.

2. Titania coating and Au decorating

The iron oxide/silica particles were extracted and dispersed in 2 mL of absolute ethanol and 10 µL of water. 2, 5, 10, and 20 µL injections of titanium (IV) *tert*-butoxide (TTB, 97%) were added under argon atmosphere in 2 mL of ethanol solution. The TTB ethanolic solution was then added to the iron oxide/silica solution to directly coat a layer of TiO_2 onto the surface of the Fe_2O_3-SiO_2 particles. Mixing continued for about 16 h. Afterward the particles were washed in absolute ethanol, then ethanol and water (1:1), and then pure water. The iron oxide-silica-titania (FeST) particles were separated from the supernatant using a magnet. Decoration of gold nanoparticles was performed following a previously defined sol-gel method by our group,[3] resulting in the desired, novel nanomaterials for use in photocatalytic degradation experiments.

FeST particles were placed 3 mL of 1% trisodium citrate solution and stirred for 10 minutes. Then the solution was added to a 25 mL flask containing 7 mL of water. The solution was heated to 100 °C and stirred using a glass stir rod. Once the solution began to boil, 100 μL of 0.01 M chloroauric acid solution was added and stirring continued for 8 min. The solution changed from a brown color to a red-pink colored solution. The flask was then removed from heat and allowed to cool to room temperature. The gold decorated iron oxide-silica-titania (FeSTA) nanoparticles were then separated and collected using a magnet. The particles were then characterized and tested for photocatalytic efficiency.

3. Separation

After cooling, the Fe_2O_3-SiO_2-TiO_2-Au solution was placed in a conical tube and placed directly above a neodymium magnet for 30 min. The particles were allowed to re-disperse into the washing solution and were collected again using the magnet. This re-dispersion was repeated several times to remove the supernatant and/or unattached nanoparticles. The nanoparticles were extracted from the bottom of the conical tube using a micropipette for further analysis.

C. Characterization

The morphologies of the samples were examined by a scanning electron microscope (Hitachi SU8320). The samples were prepared by drop casting a 2-3 μL solution on copper grids and allowing them to dry for several hours. Energy-dispersive X-ray (EDX) spectra were collected using an Oxford XMax 150 mm^2 Crystal EDS. This was performed to evaluate the elemental composition of the nanoparticles. Light scattering and ζ-potential measurements were conducted using a Brookhaven NanoBrook ZetaPALS instrument to determine hydrodynamic radii and surface charge. These measurements were taken a several intervals during the preparation of the nanoparticles (after each layer is added). Absorbance measurements were performed with a Varian model Cary 500 scan UV-Vis-NIR Spectrophotometer to determine absorbance peaks of both the synthesized nanoparticles and the model dye. The spectra obtained from the spectrophotometer were used to determine the rate of degradation for methyl orange.

D. Monitoring/Quantification of Photocatalytic Activity

The photocatalytic activity of the synthesized iron oxide/silica-titania/gold nanoparticles was represented by the photodegradation of a model analyte, methyl orange (MO, 0.05 mM) dye, in water. The particles were extracted from solution (0.5 mL of particle solution, starting with 100 μL of stock solution in 5 mL of water) and placed in 1 mL of dye solution inside a plastic cuvette. A blank standard was also prepared for comparison of photodegradation without the presence of nanophotocatalysts. The solution was then irradiated by a 400 W mercury lamp and/or a UV lamp (135 mW/cm^2, 365 nm). The absorbance of the sample at 464 nm was measured over time in 1 h increments to measure the relative drop in concentration of the model analyte. The results of these measurements were compared to the photocatalytic activity of "as-purchased" iron oxide nanoparticles as a standard, as well as titania nanoparticles, for comparison.

III. RESULTS AND DISCUSSION

A. Synthesis and characterization of Au decorated Fe_2O_3@SiO_2/TiO_2 (FeSTA) nanoparticles

Iron oxide nanoparticles purchased from Sigma Aldrich were placed in solution and sonicated prior to characterization. The reported size distribution (determined by BET surface area measurement by Sigma-Aldrich) states that the size of the particles is less than 50 nm, but under investigation by SEM, the size distribution ranged from around 10-200 nm (Figure 1(a)). The statistical size distribution and respective surface charge of the nanoparticles is shown in Table 1. The particles also had significant agglomeration, which was able to be corrected by surfactant addition (citrate) and sonication.

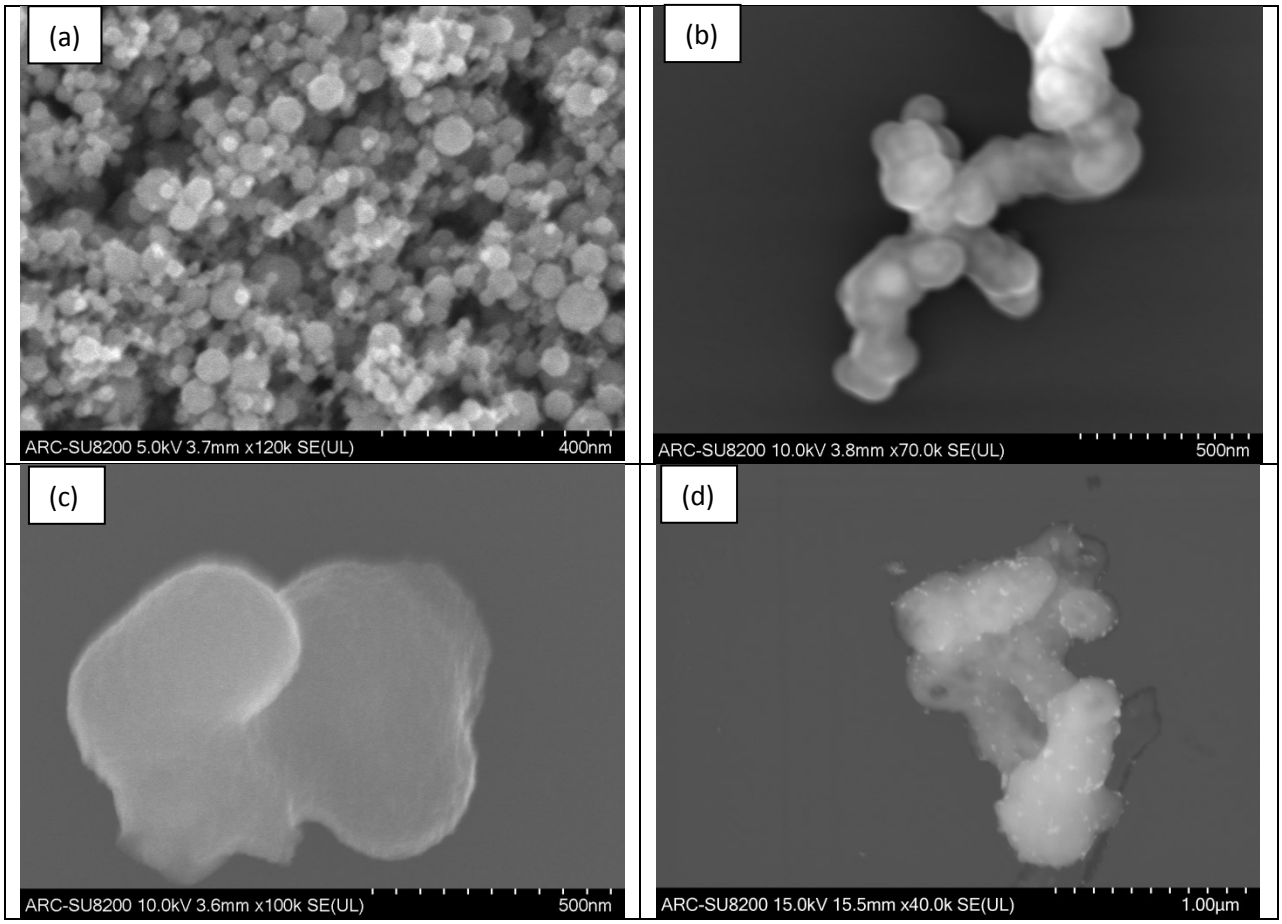

Figure 1. SEM images of nanoparticles; (a) Fe_2O_3 nanoparticles (<50 nm) purchased from Sigma Aldrich; (b) Fe_2O_3@SiO_2 nanoparticles by TEOS addition; (c) Fe_2O_3@SiO_2/TiO_2 nanoparticles by 20 µL TTB addition; (d) Au decorated Fe_2O_3@SiO_2/TiO_2 (FeSTA) nanoparticles.

Coating of the iron oxide nanoparticles with a layer of silica after citrate addition was successful. By creating a negative surface charge on the iron oxide using citrate (validated by zeta potential measurements), positively charged aqueous ammonia involved with the nucleation of silica from TEOS facilitated the attachment of silica to the citrate modified iron oxide during

hydrolysis. In Figure 1(b), the Fe_2O_3-SiO_2 (FeS) particles are shown to have a size distribution of 158 nm ± 27 nm. This significant overall increase in particle diameter could be indicative of a core-shell material, in addition to a visible difference between the center and outer region of each particle. The shell size was relatively uniform, with an average radius of 35 nm ± 10 nm. This indicates that the shell most likely surrounds more than one iron oxide nanoparticle. It is also important to note that when the ratio of ammonium hydroxide (5N) solution to ethanol was increased from 1:2 to 1:1, nanoparticle size decreased.. After silica addition, the effective surface charge of the nanoparticles was changed from -10 mV to -45 mV (Table 1), which corresponds to the high negative charge of deprotonated silanol groups in the silica shell between the pH value of 6-7.[16]

Titania precursor, titanium tert-butoxide (TTB), was placed in absolute ethanol prior to addition to the iron oxide-silica solution to prevent hydrolysis in air. The iron oxide-silica nanoparticles were then also placed in a separate ethanolic solution with a small, controlled amount of water (20 μL). This allowed for the slow condensation of TTB into solution, which formed around the silica shell. Several amounts of TTB were added to control the shell thickness and the nanoparticle sizes are shown in Table 1. The particles in Figure 1(c) are representative of the FeSTA sample (20 μL TTB added in ethanol), the largest and the sample containing the most TTB. The size distribution of the sample was 450 nm ± 76 nm. The zeta potential also changed to -9 mV, showing a significant change in surface charge around the nanoparticles. In the SEM images, a core-shell structure is not obvious, but the core-shell structure was later confirmed by energy dispersive X-ray analysis.

	Fe_2O_3	**FeS**	**FeSTA (20 uL TTB)**	**FeST2 (10 uL TTB)**	**FeST3 (5 uL TTB)**	**FeSTA4 (2 uL TTB)**
Diameter	37 nm ± 20 nm	167 nm ± 27 nm	450 nm ± 76 nm	135 nm ± 25 nm	129 nm ± 21 nm	79 nm ± 16 nm
ζ-potential	+30 mV, -10 mV w/ citrate	-45 mV	-9 mV			

Table 1. Size distribution and surface charge of nanoparticles after each additional layer is added.

Finally, gold nanospheres were decorated onto the surface of the core-shell nanomaterials by citrate reduction. The distribution of gold throughout the sample appeared to be uniform and the size of the gold nanospheres ranged from 15-22 nm (Figure 1(d)). A YAG backscattering electron (BSE) detector was used to further enhance visibility of the gold nanospheres. Images using the BSE are given in the supplementary information.

In addition to size change and surface charge analysis, elemental composition of each sample was verified using EDS. In Figure 3, spectra collected from the FeSTA sample are shown. The weight percentages of each element are also shown, with titanium having the highest percent weight of the metals. The collection of spectra was accompanied by EDX mapping to identify areas of specific elemental concentration.

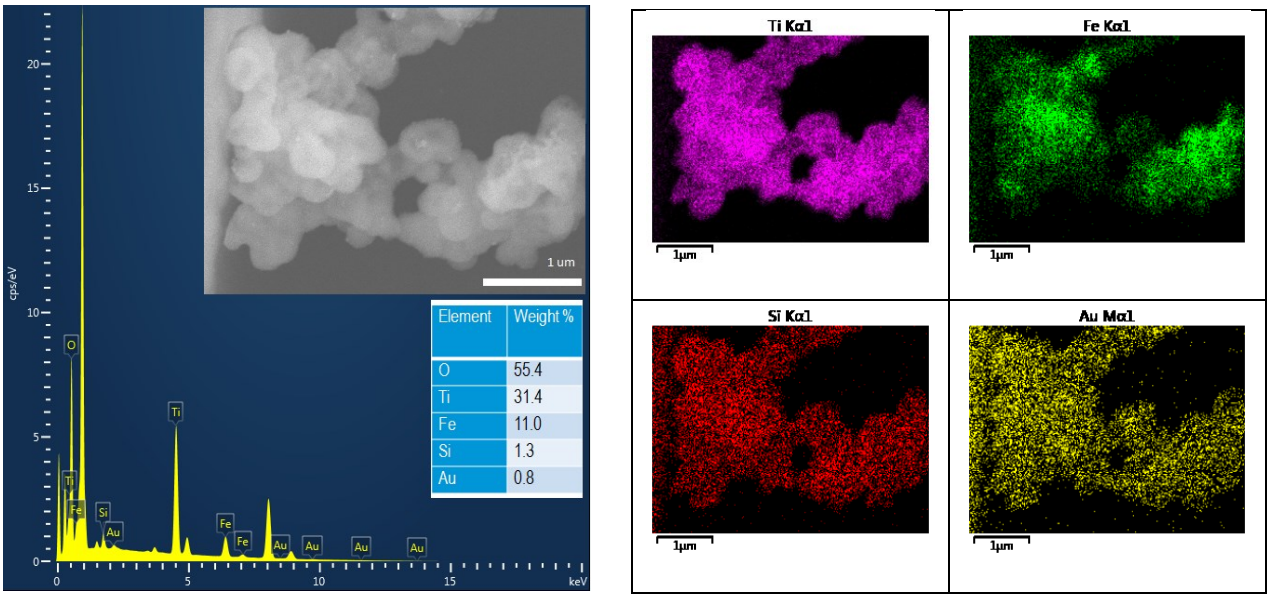

Figure 3. EDX spectrum and mapping of FeSTA nanophotocatalyst and corresponding SEM image inset and percent composition table.

B. Photocatalytic degradation of MO

The degradation of methyl orange under UV light is an advanced oxidation process (AOP) where hydroxyl radicals are produced and non-selectively break down organic compounds.[18] The mechanism by which this process occurs differs under UV and visible light, as explained by a previous study by our group.[19] Under UV light, the production of radicals is initiated by direct transitions of electrons in titania from its valence band to its conduction band. Under visible light irradiation, the electrons of the visible light absorbing components (in this case, iron oxide and gold) are transferred to the defect conduction band states of titania. This results in radical formation under both UV and visible light.

The photocatalytic activity of the prepared nanophotocatalysts was evaluated by changes in the absorbance spectrum of methyl orange and the decrease in peak absorbance at 464 nm (Figure 5). This wavelength was reported to be the specific value that gives the compound an orange color.[20,21] The experiment was performed at ambient temperature. A solution of methyl orange exposed to UV illumination without catalysts and was used as a control to evaluate MO's behavior in the absence of a catalyst. The synthesized nanoparticles with the largest titania shell thickness (FeSTA) were tested under UV irradiation only.

In Figure 4, the UV-Vis absorbance spectra of several UV photodegradation experiments are shown. There is a small decrease in absorbance for the control solution of methyl orange but this decrease occurred within the first hour of UV light exposure and did not continue after prolonged exposure for an additional five hours. This effect could be due to the natural breakdown of dyes under UV irradiation. Similarly, iron (III) oxide nanoparticles purchased from Sigma Aldrich did not influence the photocatalytic breakdown of MO under UV light. This was expected because of the weak absorption of iron oxide in the UV range. However, the 25 nm titania nanoparticles were successful in reducing the MO absorption peak by 83% in two hours and more than 90% after 5 hours. When the prepared nanophotocatalysts (FeSTA) were tested, the reduction in the

464 nm peak was 84% after five hours. The exact concentration required for this degradation is not known, but is still under investigation and will be reported at a later date.

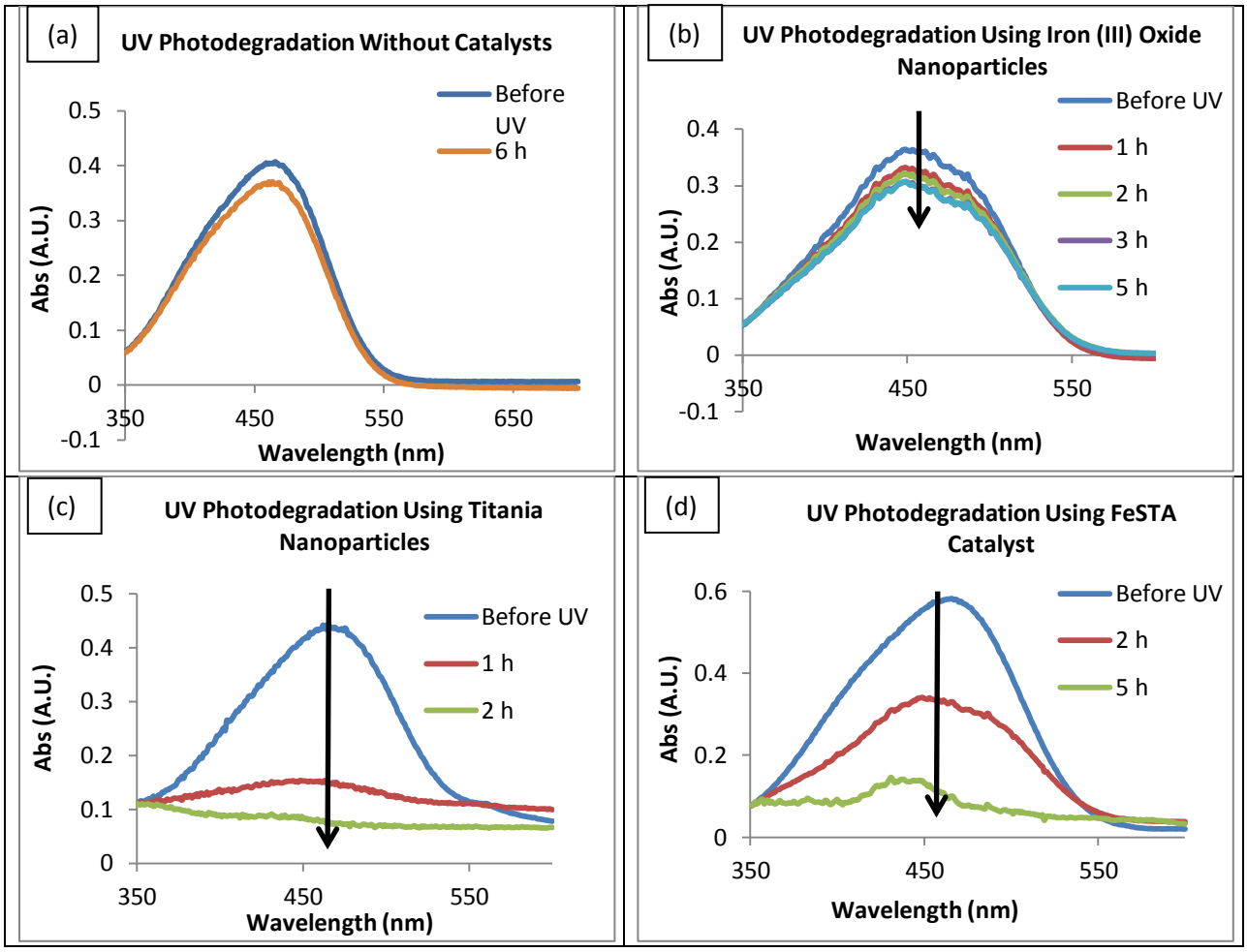

Figure 4. UV-Vis absorbance spectra of methyl orange under UV illumination; (a) without catalysts; (b) with iron (III) oxide nanoparticles; (c) with titania nanoparticles; (d) with FeSTA nanophotocatalysts.

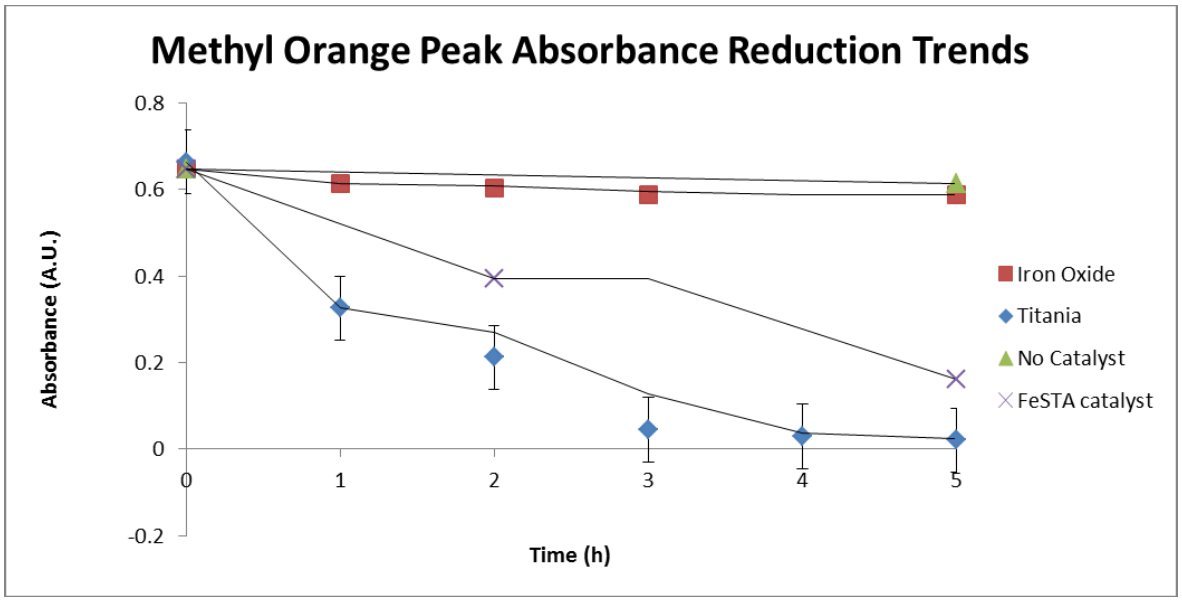

Figure 5. Reduction of MO peak absorbance at 464 nm under UV illumination over 5 hours using different nanophotocatalysts.

CONCLUSIONS

This study shows the successful preparation, characterization, and testing of a novel photocatalytic material that is active in both the UV and visible range. The well dispersed iron (III) oxide core nanospheres were treated by the hydrolysis and condensation of TEOS. A similar process was used to produce an additional titania shell with varying thickness by condensation of different amounts of TTB at the surface of the Fe_2O_3@SiO_2 nanoparticles. Finally, the monodispersed, stable Fe_2O_3@SiO_2/TiO_2 nanoparticles were decorated with 20 nm gold spheres by citrate reduction. The composite nanomaterials were then compared to other nanophotocatalysts. The photocatalytic activity of the novel nanomaterial resulted in a peak absorbance reduction of 84% after 5 hours of UV light exposure. Further testing is required to determine the quantity of enhancement by visible light irradiation and the effect of titania shell thickness on photocatalytic activity.

IV. ACKNOWLEDGMENTS

We would like to thank Savannah River National Lab (United States of America, DOE) and Aiken County for funding and use of equipment, respectively. This work was supported in part by the U.S. Department of Energy, Office of Science, Office of Workforce Development for Teachers and Scientists (WDTS) under the Science Undergraduate Laboratory Internships Program (SULI).

V. REFERENCES

[1]Pankaj Chowdhury, Hassan Gomaa, Ajay K. Ray, "Dye-Sensitized Photocatalyst: A Breakthrough in Green Energy and Environmental Detoxification," Sustainable Nanotechnology and the Environment: Advances and Achievements, (231-266) (2013).

[2]Meidan Ye, in *Low-cost Nanomaterials: Toward Greener and More Efficient Energy Applications*, edited by Zhiqun Lin, Jun Wang (2014), pp. 9-17.

[3]Murph, S. E. H., Larsen, G. K., Lascola, R. J. "Multifunctional Hybrid Fe_2O_3-Au Nanoparticles for Efficient Plasmonic Heating," J. Vis. Exp. (108), (2016).

[4]Ravi Kumar Gautam, Mahesh Chandra, in *Nanomaterials for Wastewater Remediation*, edited by Peter Jardim (Cambridge, MA, 2016), pp. 2-18.

[5]Landong Li, Junqing Yan, Tuo Wang, Zhi-Jian Zhao, Jinlong Gong, Naijia Guan, "Sub-10 nm rutile titanium dioxide nanoparticles for efficient visible-light-driven photocatalytic hydrogen production," Nature Comm. 6, 5881 (2015).

[6]Wang, J. L., "Advanced Oxidation Processes for Wastewater Treatment: Formation of Hydroxyl Radical and Application," Critical Reviews in Environmental Science and Technology 42, (2012).

[7]Pelaez, M. et al, "A Review on the Visible Light Active Titanium Dioxide Photocatalysts for Environmental Applications," Applied Catalysis B: Environmental 125, p. 331– 349 (2012).

[8]Li, Y. in *Green Carbon Dioxide: Advances in CO Utilization*, edited by G. Centi and S. Perathoner (Hoboken, NJ, USA, 2014).

[9]Ariel L. Cappelletti. et al, "Synthesis, Characterization, and Nanocatalysis Application of Core–Shell Superparamagnetic Nanoparticles of Fe_3O_4@Pd," Australian J. of Chem. 68 (10), 1492-1501 (2015).

[10]Rajesh Chalasani, Sukumaran Vasudevan, "Cyclodextrin-Functionalized Fe3O4@TiO2: Reusable, Magnetic Nanoparticles for Photocatalytic Degradation of Endocrine-Disrupting Chemicals in Water Supplies," ACS Nano 7 (5), 4093–4104 (2013).

[11]N. Seriani, C. Pinilla, S. Cereda, A. De Vita, S. Scandolo, "Titania−Silica Interfaces," J. Phys. Chem. C 116 (20), 11062–11067 (2012).

[12]Vishal N. Koparde, Peter T. Cummings, "Molecular Dynamics Simulation of Titanium Dioxide Nanoparticle Sintering," J. Phys. Chem. B 109, 24280-24287 (2005).

[13]Yuanchao Zhang, Wendy Chu, Alireza Dibaji Foroushani, Hongbin Wang, Da Li, Jingquan Liu, Colin J. Barrow, Xin Wang, Wenrong Yang, "New Gold Nanostructures for Sensor Applications: A Review," Materials 7, 5169-5201 (2014).

[14]Jongmin Kim, Hongsik Choi, Changwoo Nahm, Byungwoo Park, "Surface-plasmon resonance for photoluminescence and solar-cell applications," Electronic Materials Letters 8 (4), 351-364 (2012).

[15]Stefan A. Meyer, Eric C. Le Ru, Pablo G. Etchegoin, "Combining Surface Plasmon Resonance (SPR) Spectroscopy with Surface-Enhanced Raman Scattering (SERS)," Anal. Chem. 83 (6), 2337–2344 (2011).

[16]Suh Cem Pang, Sze Yun Kho, and Suk Fun Chin, "Fabrication of Magnetite/Silica/Titania Core-Shell Nanoparticles," Journal of Nanomaterials, (2012).

[17]Hunyadi, S.E. and Murphy, C.J., "Tunable One-Dimensional Silver-Silica Nanopeapod Architectures," J. Phys. Chem. B 110, 7226-7231 (2006).

[18]Wang, X. and Caruso, R., "Enhancing photocatalytic activity of titania materials by using porous structures and the addition of gold nanoparticles," J. Mater. Chem. 21, 20-28 (2010).

[19]Zyoud A., et. al, "Optimizing photo-mineralization of aqueous methyl orange by nano-ZnO catalyst under simulated natural conditions," J. Environ. Health Sci. Eng. 13, 46 (2015).

[20]Murph, S., "One-dimensional plasmonic nano-photocatalysts: synthesis, characterization and photocatalytic activity," Solar Hydrogen and Nanotechnology VI, 8109 (2011).

[21]Sait Elmas, Filip Ambroz, Dipankar Chugh, and Thomas Nann, "Microfluidic Chip for the Photocatalytic Production of Active Chlorine," Langmuir 32 (19), 4952–4958 (2016).

[22]Shenghui X., Ping Huang, Jamie J. Kruzic, Xierong Zeng, and Haixia Qian, "A highly efficient degradation mechanism of methyl orange using Fe-based metallic glass powders," Sci Rep. 6, 21947 (2016).

[23] John Buffo, Leo J. Fritschen, James L. Murphy, "Direct Solar Radiation On Various Slopes From 0 To 60 Degrees North Latitude," Pacific Northwest Forest and Range Experiment Station, Forest Service, U.S. Department of Agriculture, Portland, Oregon,USA (1976).

[24]Chaudhuri, R. G. and Paria, S. "Core/Shell Nanoparticles: Classes, Properties, Synthesis Mechanisms, Characterization, and Applications," Chemical Reviews 112 (4), 2373-433 (2011).

[25] Kowalska E., Mahaney O., Abe R., Ohtani B., "Visible-light-induced photocatalysis through surface plasmon excitation of gold on titania surfaces," Phys Chem Chem Phys. 12 (10), 2344-55 (2010).

SUPPLEMENTARY INFORMATION

Three samples of iron oxide-silica-titania nanoparticles with different amounts of titanium tert-butoxide precursor (2, 5, 10 uL), SEM images and size distribution histograms.

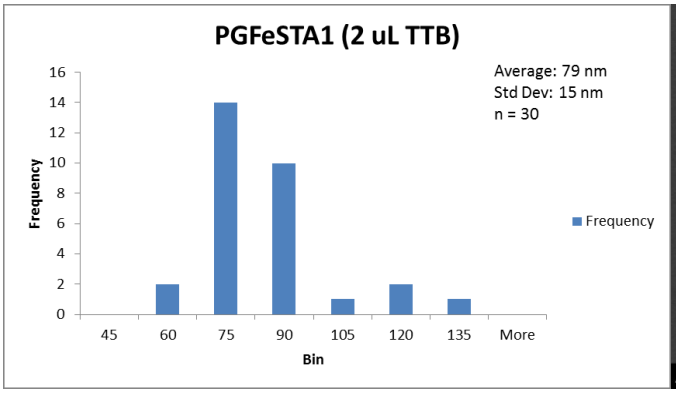

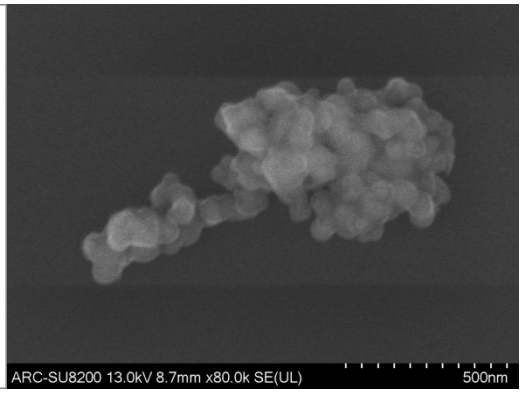

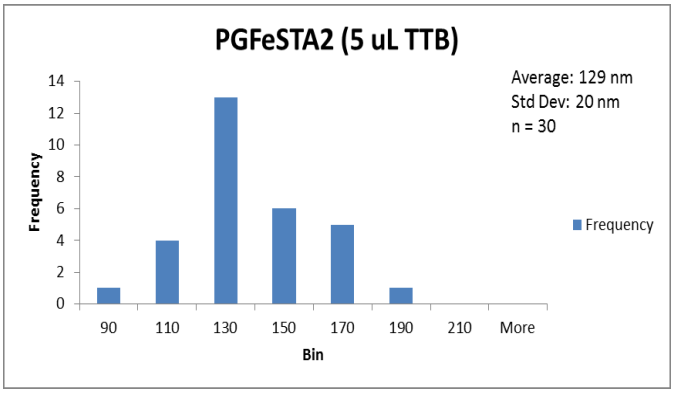

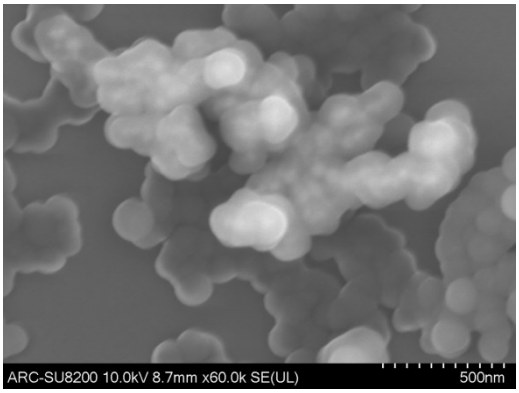

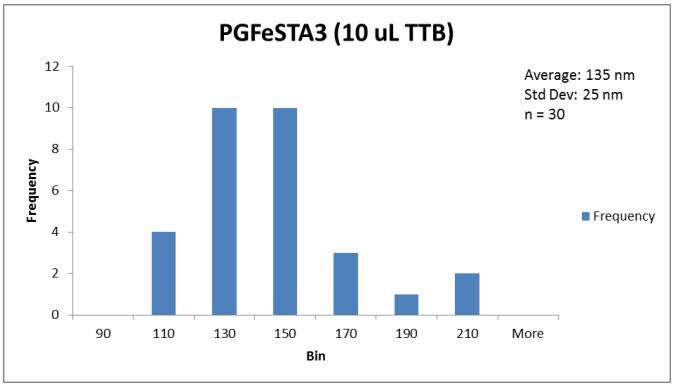

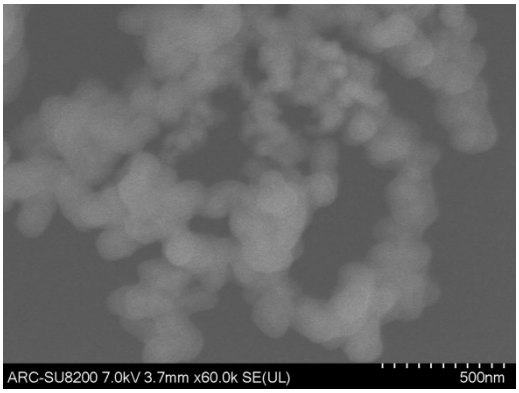

FeSTA Nanoparticles (20 uL of TTB):

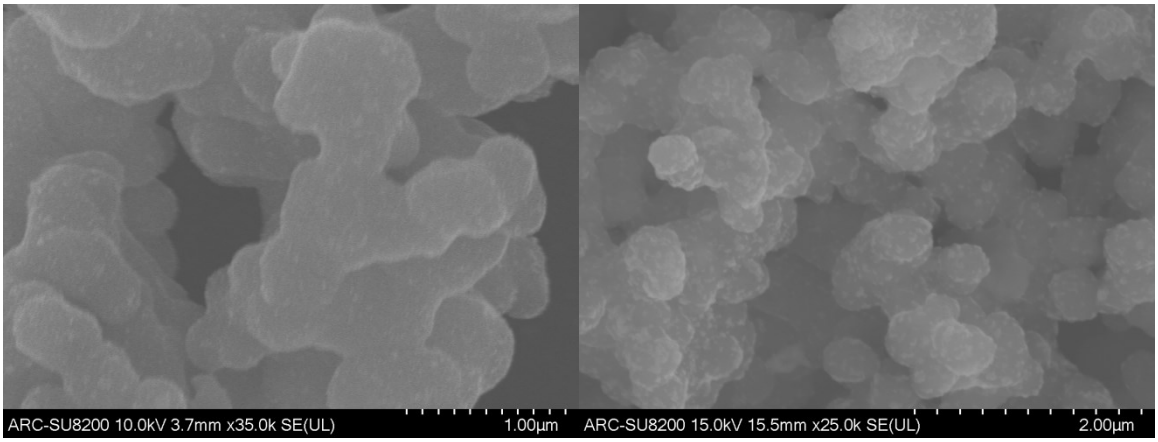

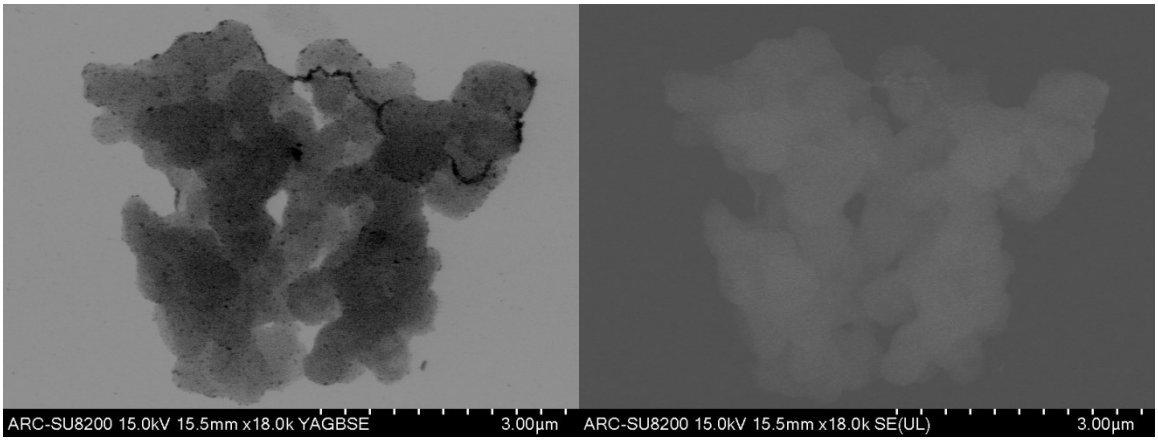

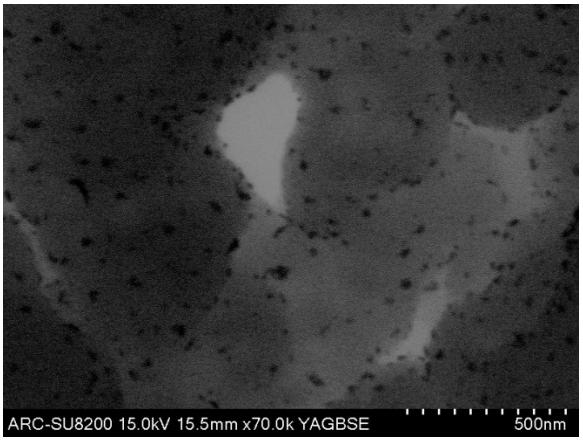

FeSTA, before gold addition (iron oxide-silica-titania):

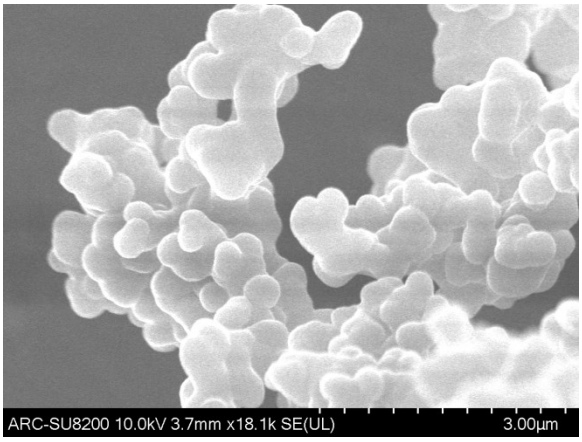

FeSTA, before titania addition (iron oxide-silica):

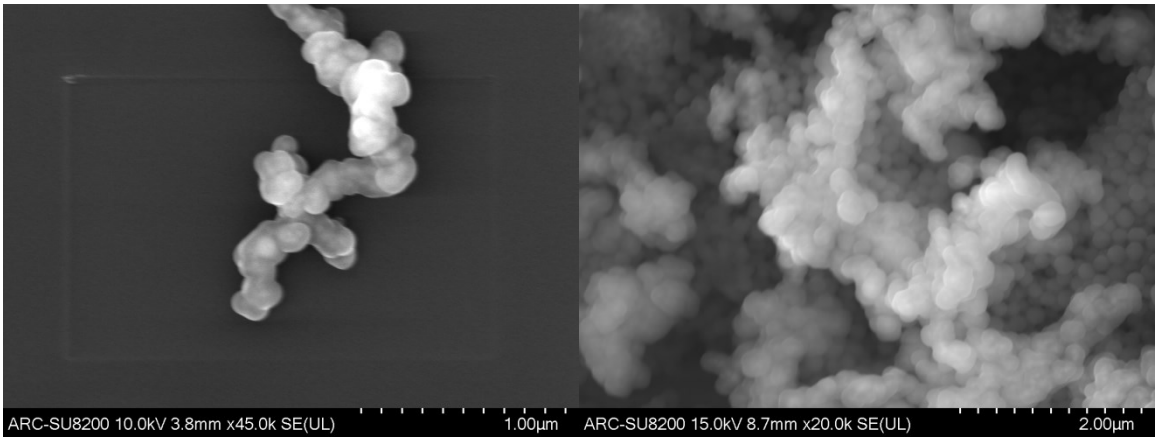

FeSTA, before silica addition (iron (III) oxide):